

Shell evolution from $N = 34$ towards $N = 40$: first 2^+ state in ^{52}Ar and the second 0^+ state in ^{54}Ca

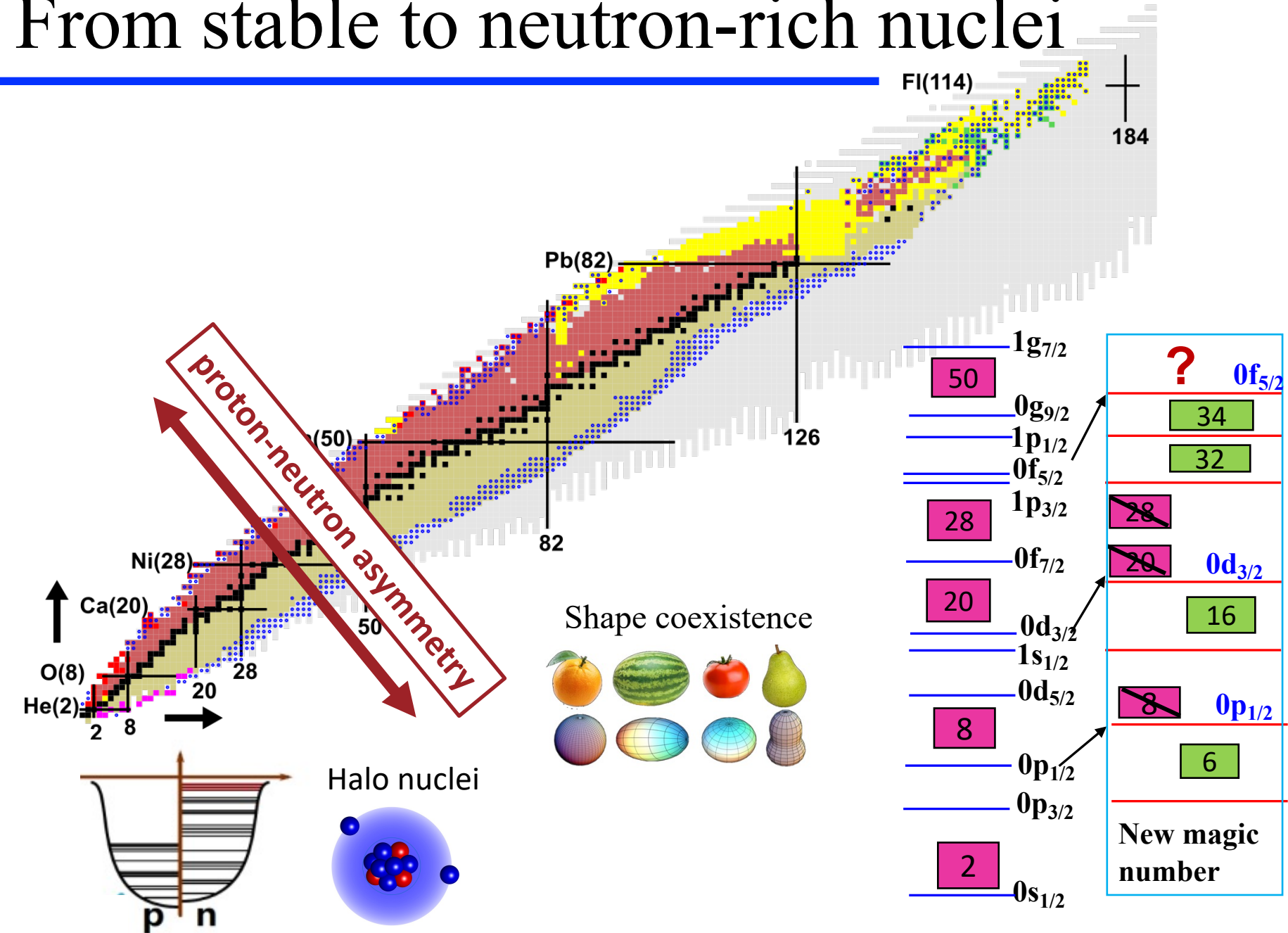
Hongna Liu

Beijing Normal University

DREB2022, 26 June-1 July 2022, Santiago de Compostela

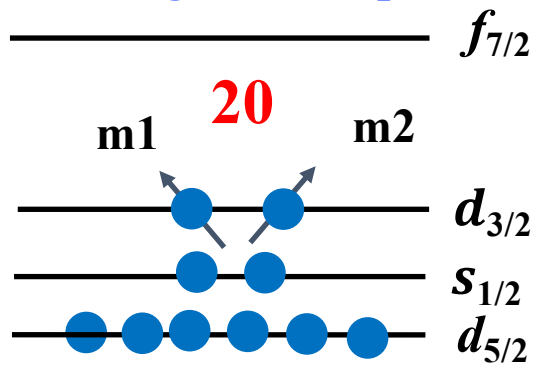


From stable to neutron-rich nuclei



Indicator of Shell Closure: Systematics of E(2_1^+)

Rearrangement of particles

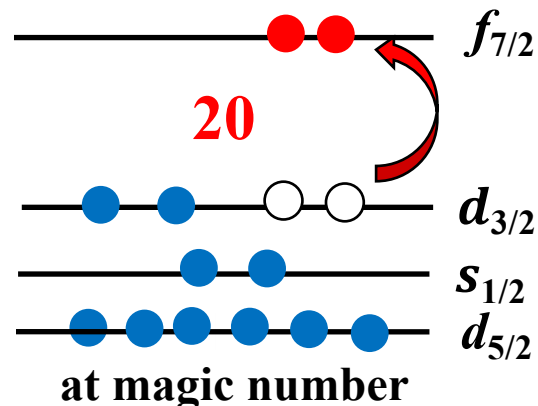


Open shell

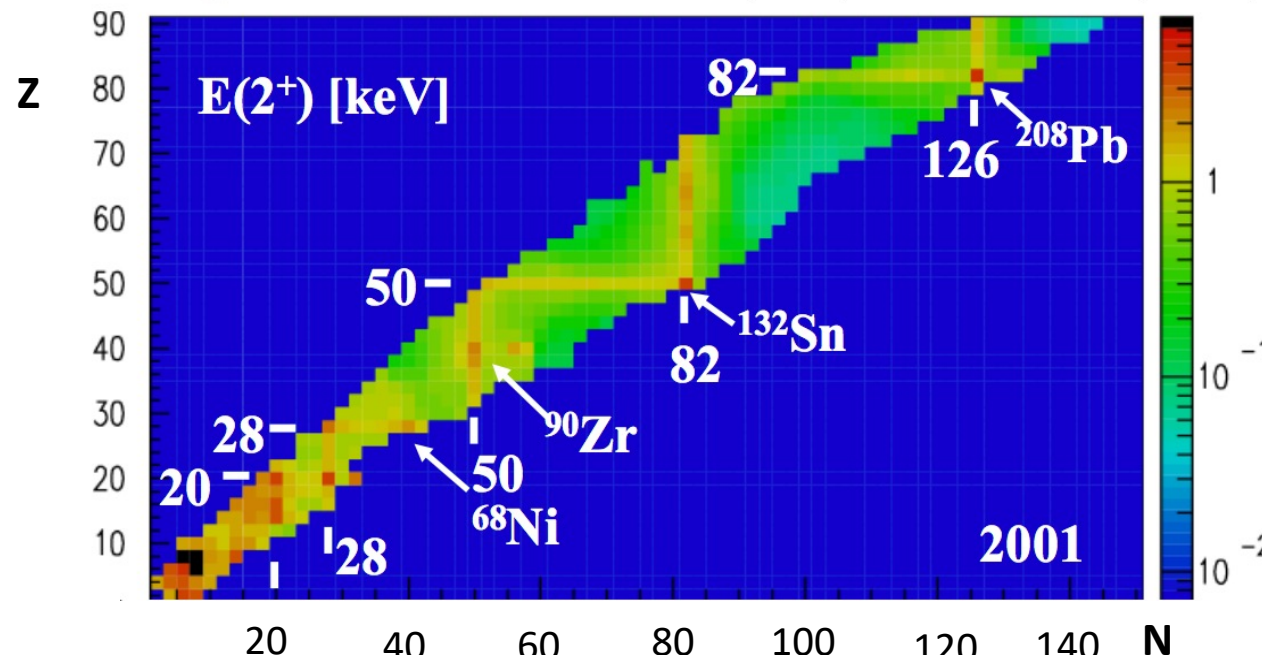
Configuration of 2_1^+

$f_{7/2}$

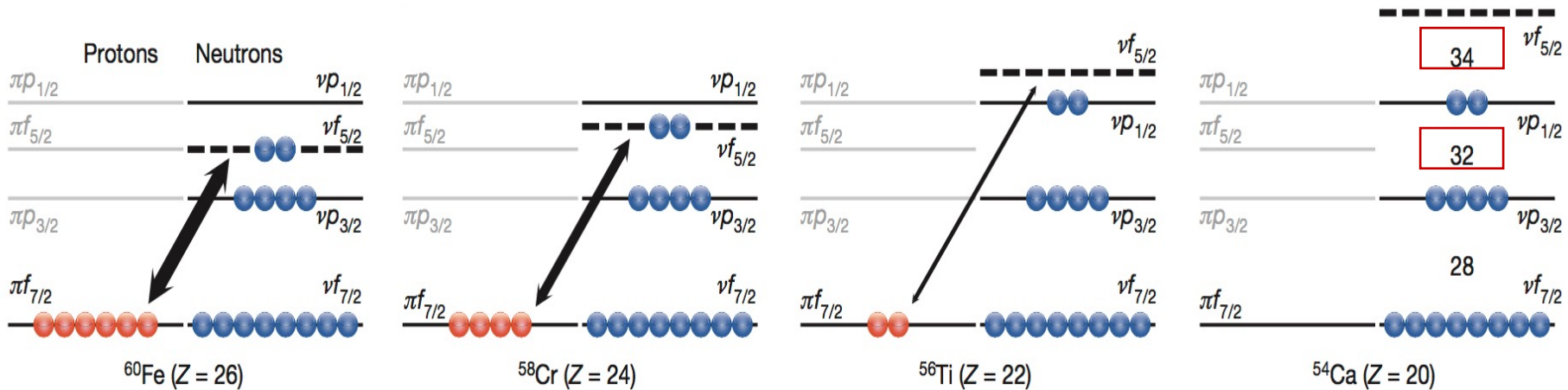
Cross-shell excitation



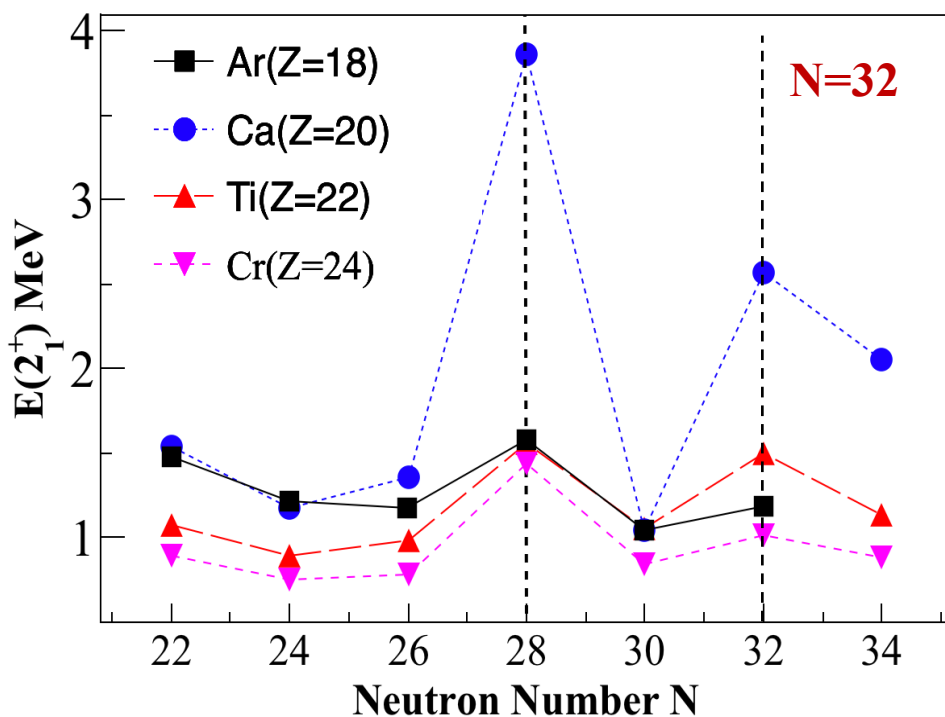
Closed shell



New subshell closures around A~50

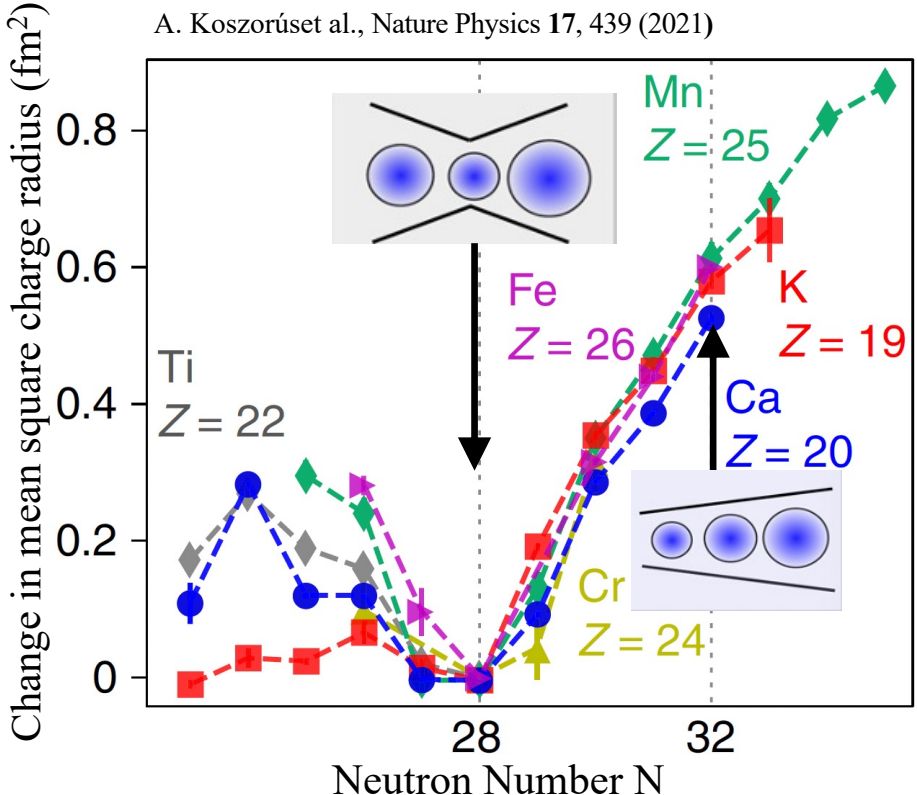


D. S. et al, Nature 502 (2013)

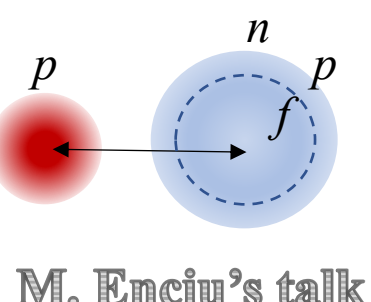
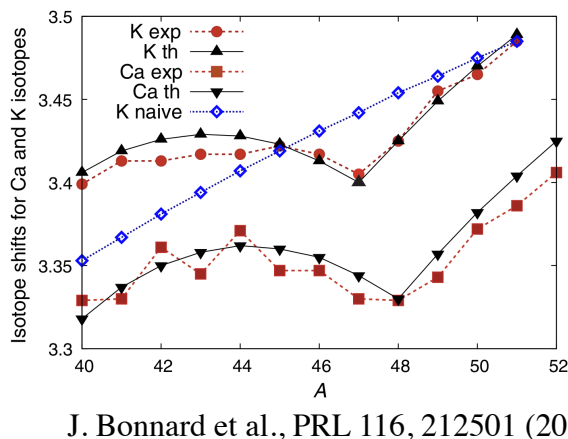
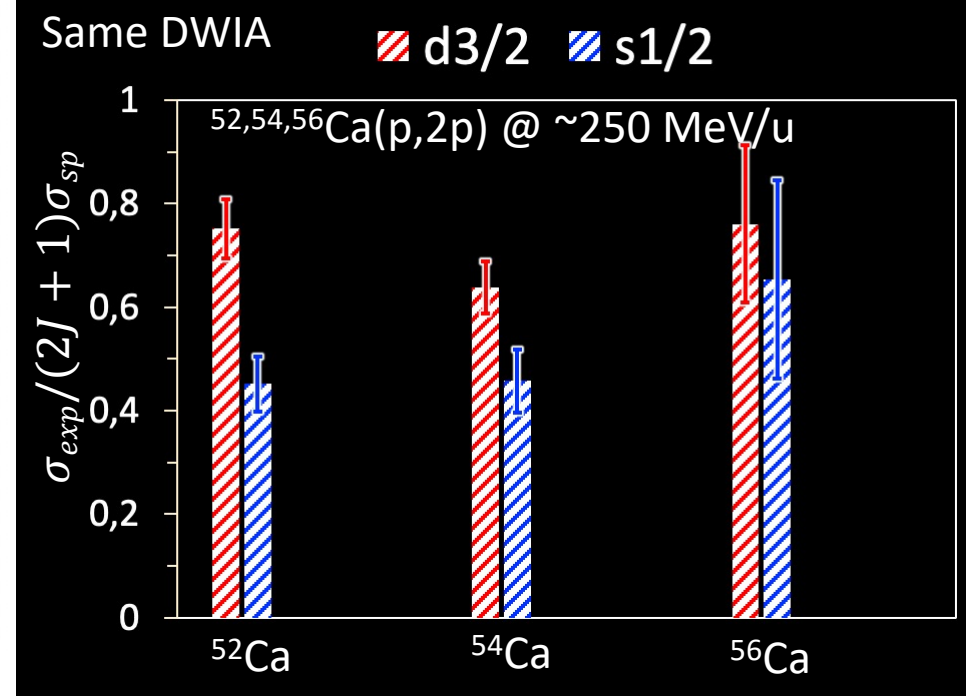


Unexpected large Charge radius at N = 32

A. Koszorúset al., Nature Physics 17, 439 (2021)

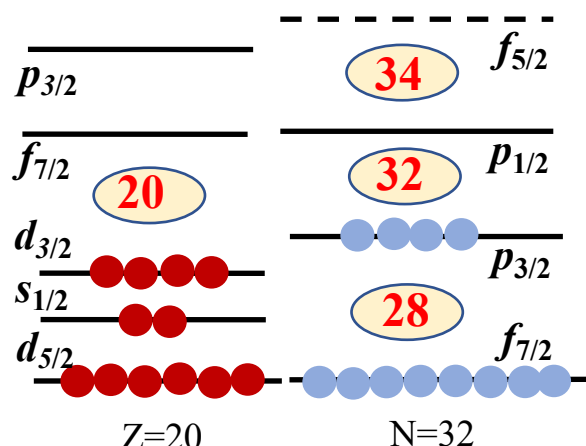


Y. L. Sun et al, PLB 802, 135215(2020); K. Wimmer et al., PLB 827, 136953 (2022)

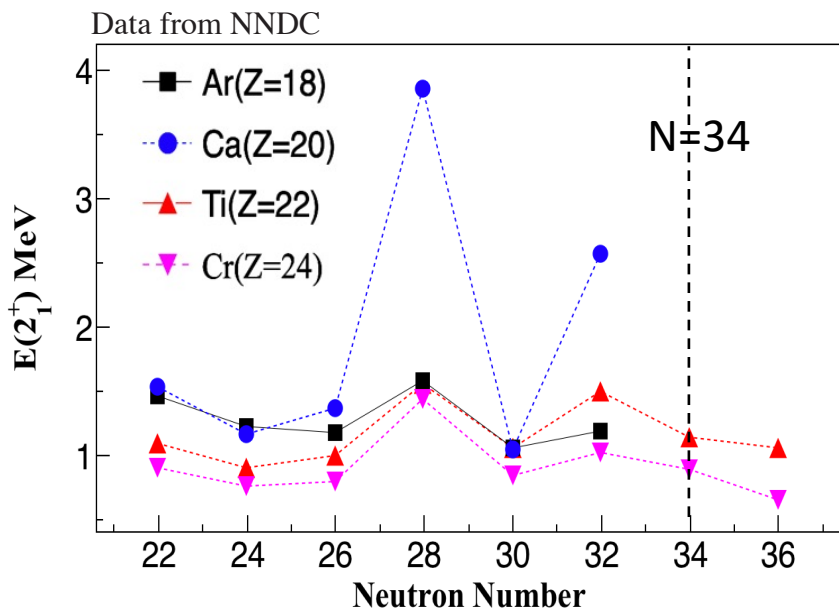


M. Enciu's talk

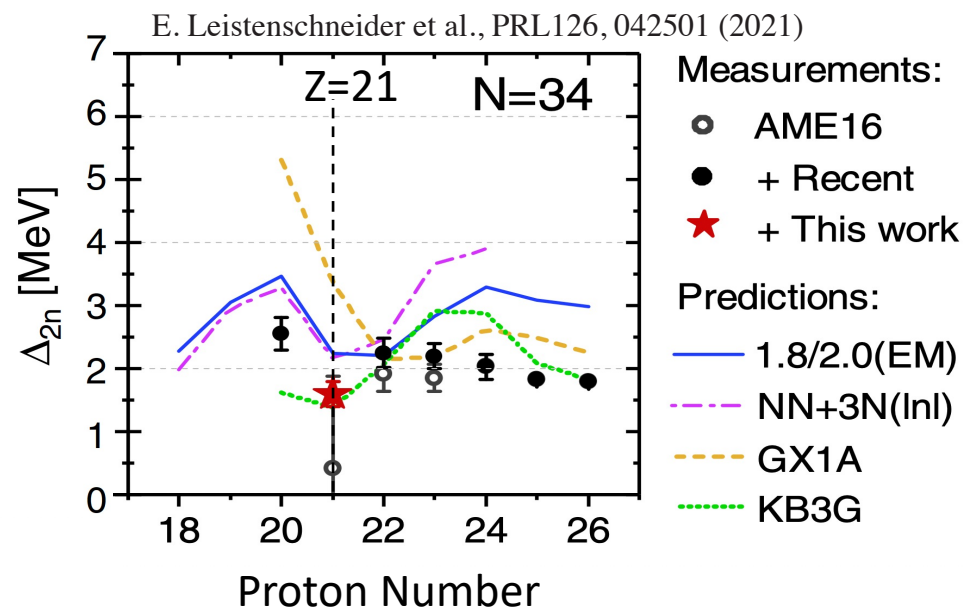
J. Bonnard et al., PRL 116, 212501 (2016)



Is N=34 a new sub-shell closure?



Mass measurement of
D. Steffenbeck et al., PRC 96(2017) 064310

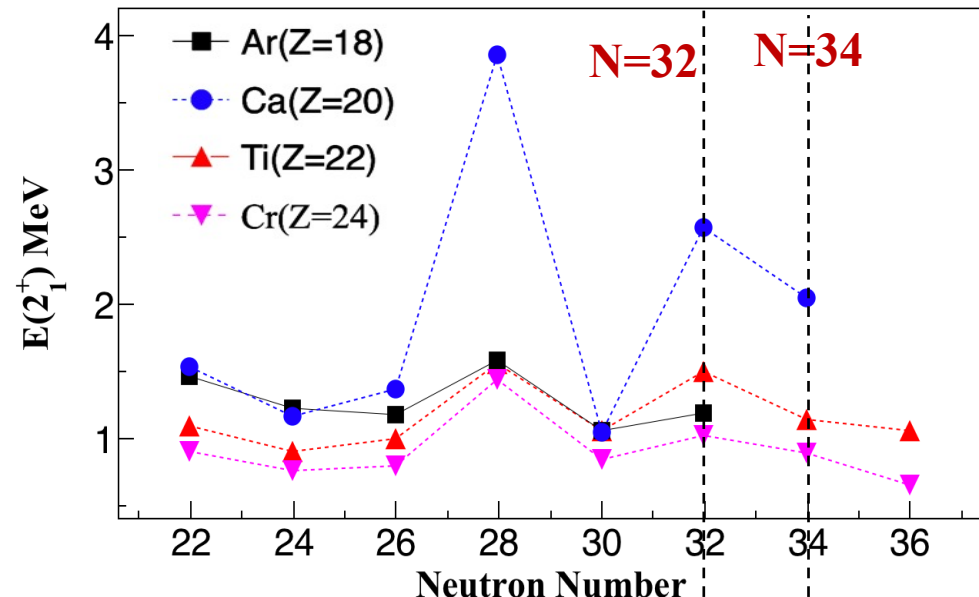


Excitation energy of the negative parity state in ^{55}Sc
D. Steffenbeck et al., PRC 96(2017) 064310

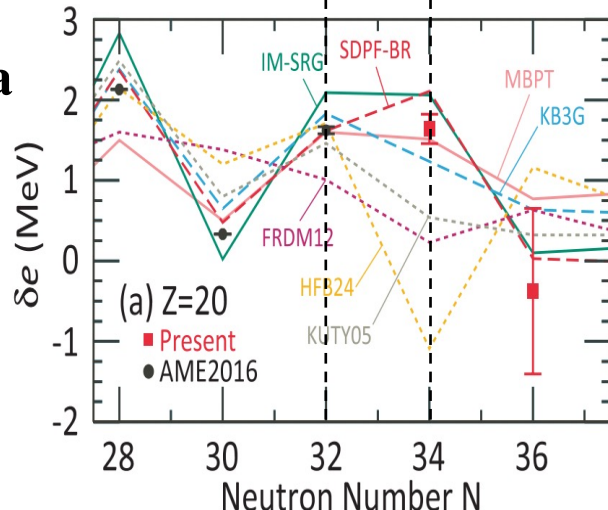
Non-closed N = 34 subshell closure for nuclei with Z > 20

A sizable N=34 subshell closure in ^{54}Ca

D. Steffenbeck et al, Nature 502 (2013)

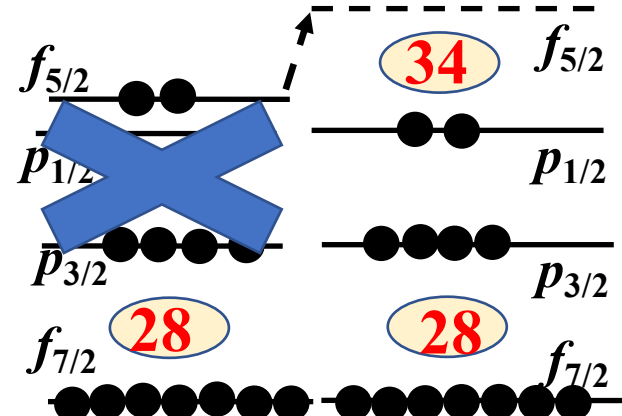


Mass of $^{55-57}\text{Ca}$

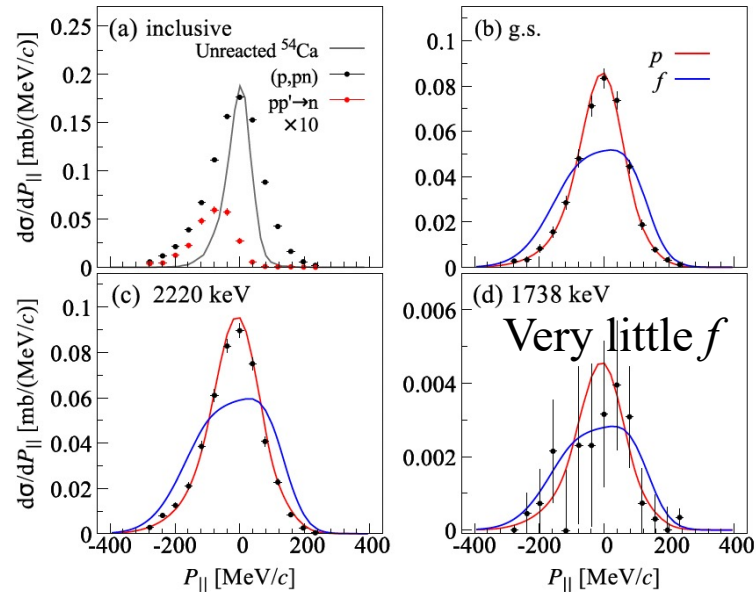


S. Michimasa et al. Phys. Rev. Lett. 121, 022506 (2018)

$^{54}\text{Ca}(p,pn)^{53}\text{Ca}$



S. Chen et al. Phys. Rev. Lett. 123, 142501 (2019)

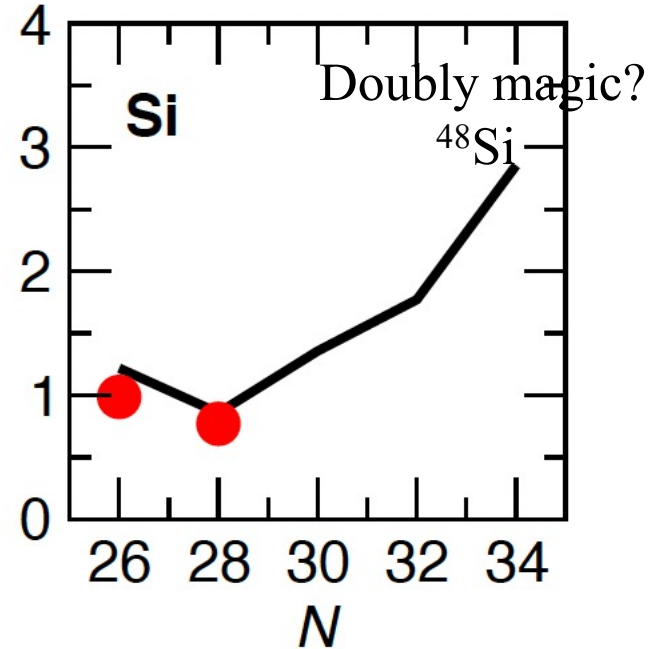
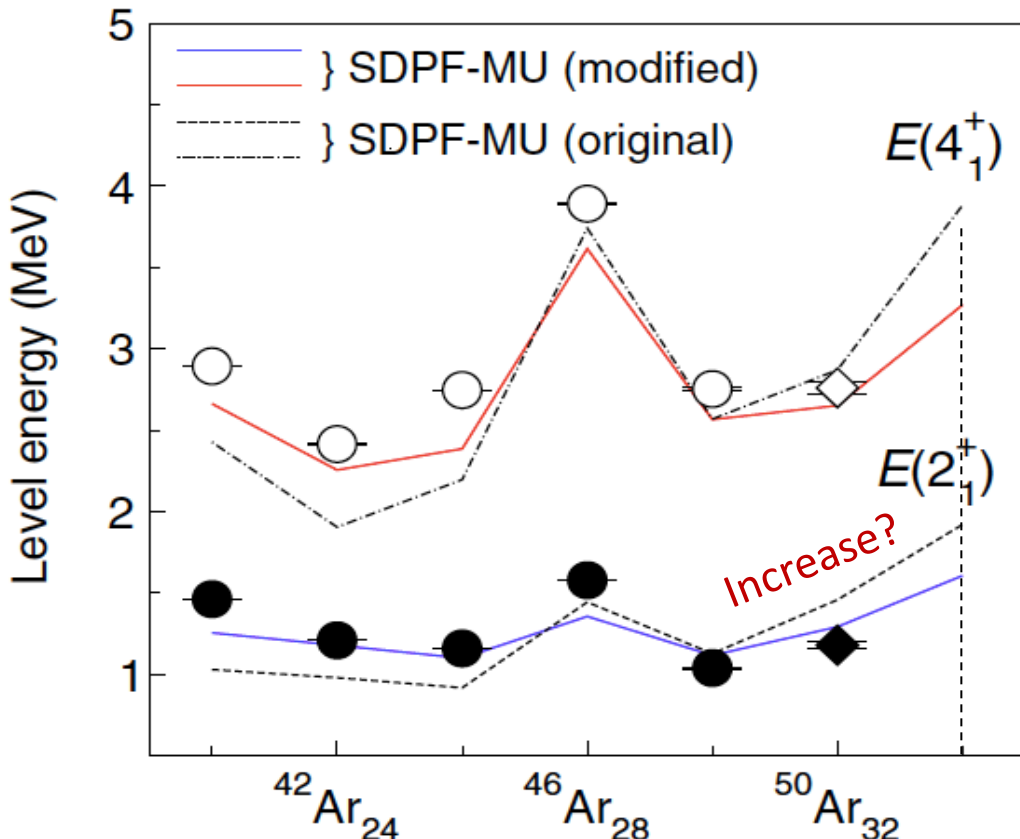


Robustness of the N=34 sub-shell for Z<20

Y. Utsuno et al, JPS Conf. Proc. 6, 010007 (2015).

Shell gaps predicted by SDPF-MU

	Ti	Ca	Ar
$N = 32$	2.54 MeV	2.43 MeV	2.27 MeV
$N = 34$	1.77 MeV	2.64 MeV	3.13 MeV



Goal of this work:
Measure the excitation energy of
the low-lying states of ^{52}Ar .

At present, ^{52}Ar is the most
neutron-rich N=34 nucleus
accessible by experiment.

D. S. et al., PRL 114, 252501 (2015)

Beyond ^{54}Ca : first spectroscopy of ^{52}Ar ($Z=18$)



^{70}Zn beam 345MeV/u 200~250pnA

^{53}K intensity: 1.0 pps ;

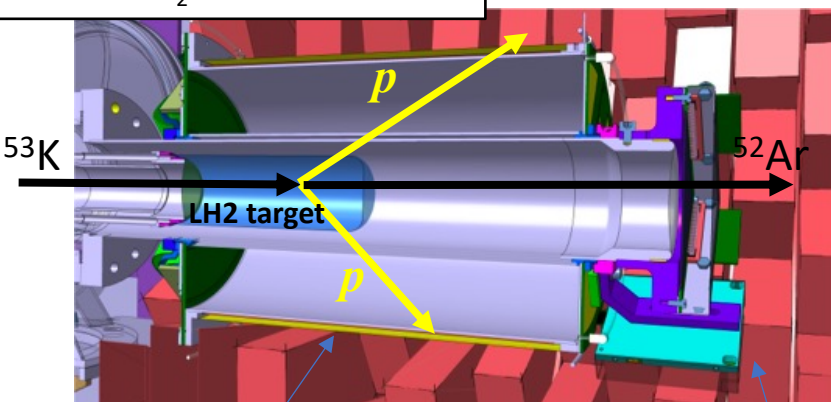
$^{53}\text{K}(\text{p},\text{p})^{52}\text{Ar}$ @ 240 MeV/nucleon

150mm liquid hydrogen (LH_2) target

Improve the luminosity by a factor of ~ 5

7 day beam time: 438 counts of ^{52}Ar

MINOS: $\text{LH}_2 + \text{vertex tracker}$



Vertex tracker: TPC

DALI2+: NaI(Tl) array

DALI2+: 226 detectors

Efficiency: 30% @ 1MeV

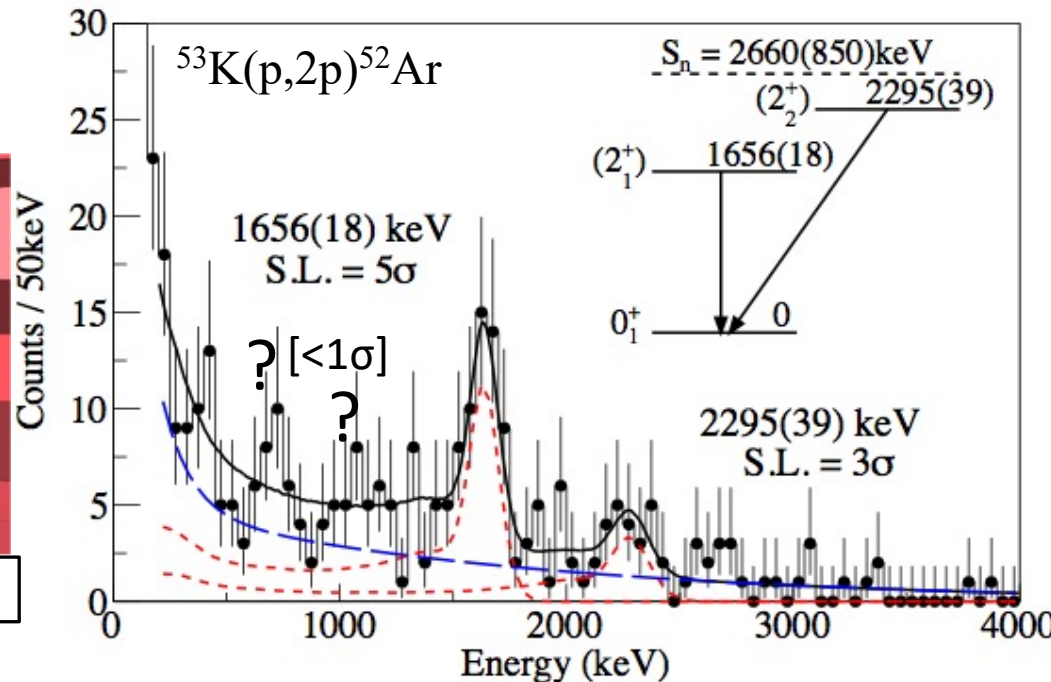
Resolution: 10% @1MeV

^{54}Ca : Exp. $S_n = 3840(70)$ keV

^{52}Ar : $S_n = 2660(850)$ keV

F. Wienholtz et al., Nature 498, 346(2013)

AME, Chinese Physics C Vol. 41, No. 3 (2017)

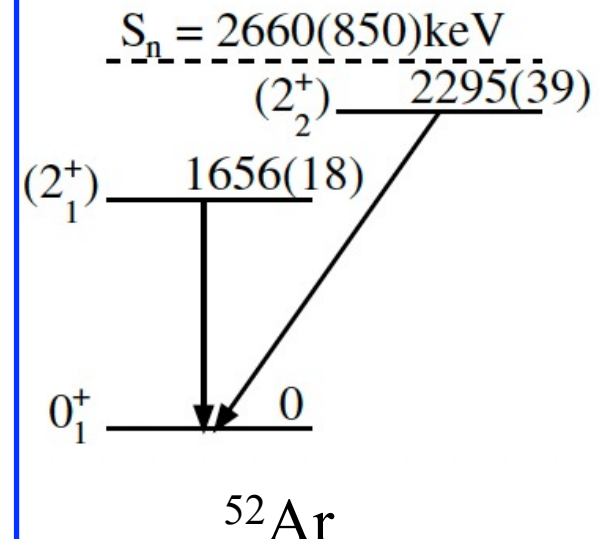


Fitting function: Simulated response function +
bg. shape for $^{51}\text{K}(\text{p},\text{p})^{50}\text{Ar}$

Energy level scheme of ^{52}Ar

*Only list states lying below S_n with $C^2S > 0.01$

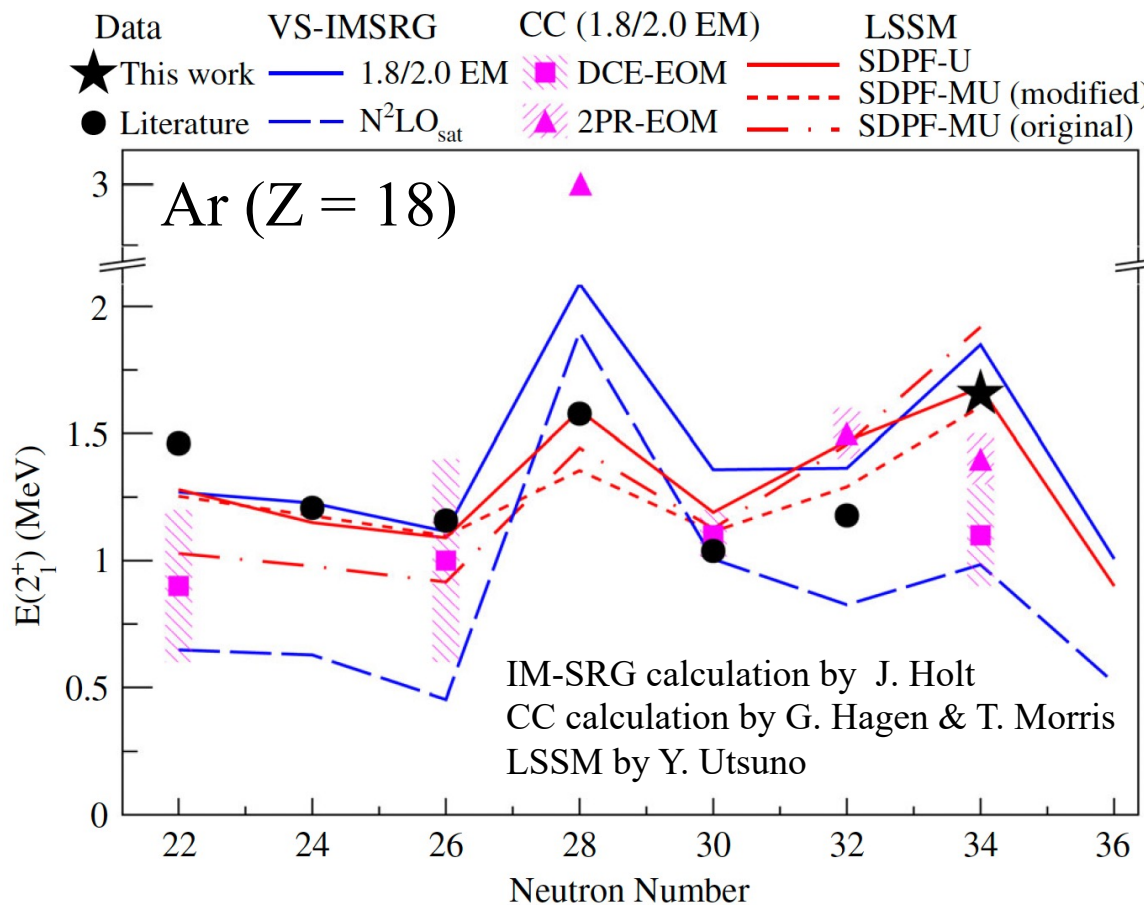
Experiment		Theory					
E_{exp} (keV)	σ_{exp} (mb)	E_x (keV)	J^π	l_j	$C^2 S_{\text{th}}$	$\langle \sigma_{\text{sp}} \rangle$ (mb)	σ_{th} (mb)
0	0.7(3) ^a	0	0_1^+	$d_{3/2}$	0.28	3.03	0.86
1656(18)	0.9(2)	1849	2_1^+	$s_{1/2}$	0.10	0.92	1.13
				$d_{3/2}$	0.33	2.94	
				$d_{5/2}$	0.02	4.82	
2295(39)	0.4(1)	1974	0_2^+	$d_{3/2}$	0.01	2.93	0.04
		2367	2_2^+	$s_{1/2}$	0.13	0.92	0.30
				$d_{3/2}$	0.05	2.91	
				$d_{5/2}$	0.01	4.76	
Inclusive	1.9(1)						2.32



IM-SRG calculation with 1.8/2.0 EM interaction by J. Holt
Eikonal calculation by C. A. Bertulani

The peak at 1.7 MeV is assigned to be the transition $2_1^+ \rightarrow 0_1^+$ of ^{52}Ar .

Comparison with theoretical calculations

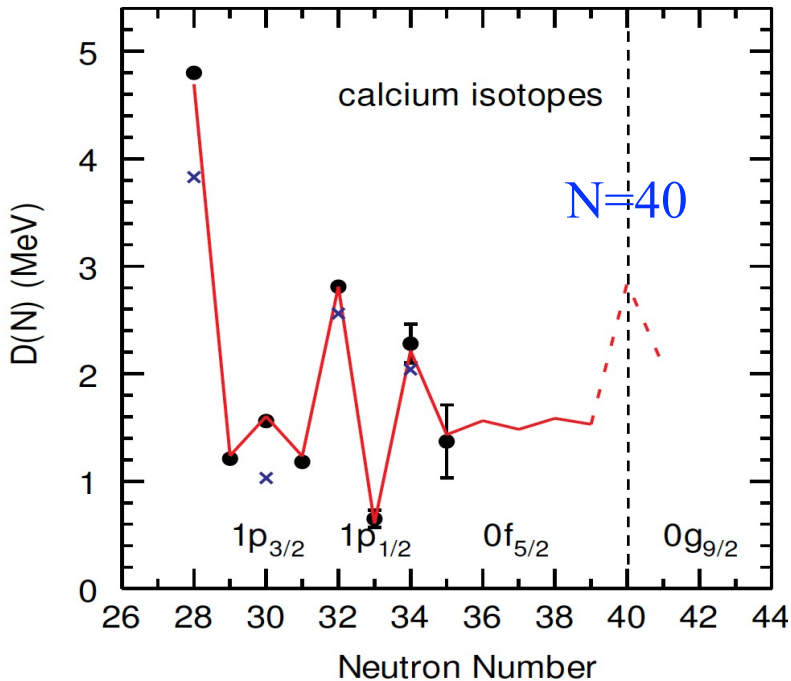


$E(2_1^+)$ is max. at $N=34$, greater than that at $N=32$ and $N=28$.

→ A significant $N=34$ subshell closure was observed in ^{52}Ar ($Z<20$).

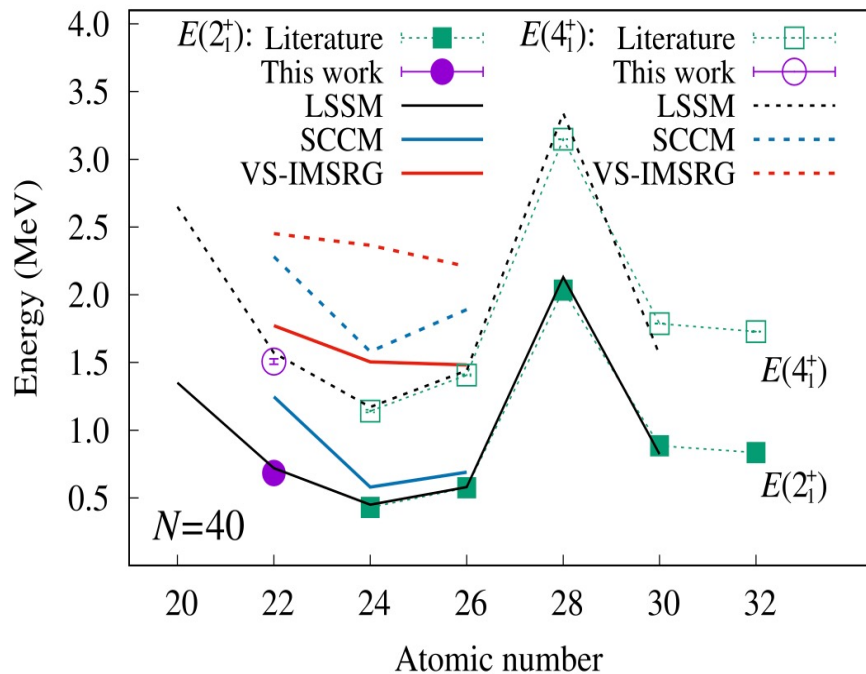
Shell evolution beyond N = 34

$$D(q) = (-1)^q [2\text{BE}(q) - \text{BE}(q+1) - \text{BE}(q-1)]$$



B. A. Brown, Physics 2022, 4, 525–547.

M.L. Cortés et al., PLB 800 (2020) 135071.



Valence neutron occupancy in ^{60}Ca

Interaction	J^π	$0f_{5/2}$	$0g_{9/2}$	$1d_{5/2}$
LNPS-U	0 ⁺	3.05	2.38	Intruder
M+P		3.42	2.11	0.83
LNPS-U	2 ⁺	2.60	2.47	1.36
M+P		3.40	1.76	1.10
LNPS-U	4 ⁺	2.57	2.46	1.32
M+P		3.40	1.76	1.10

F. Nowacki, A. Obertelli and A. Poves, Progress in Particle and Nuclear Physics 120 (2021) 103866.

See Chen's talk

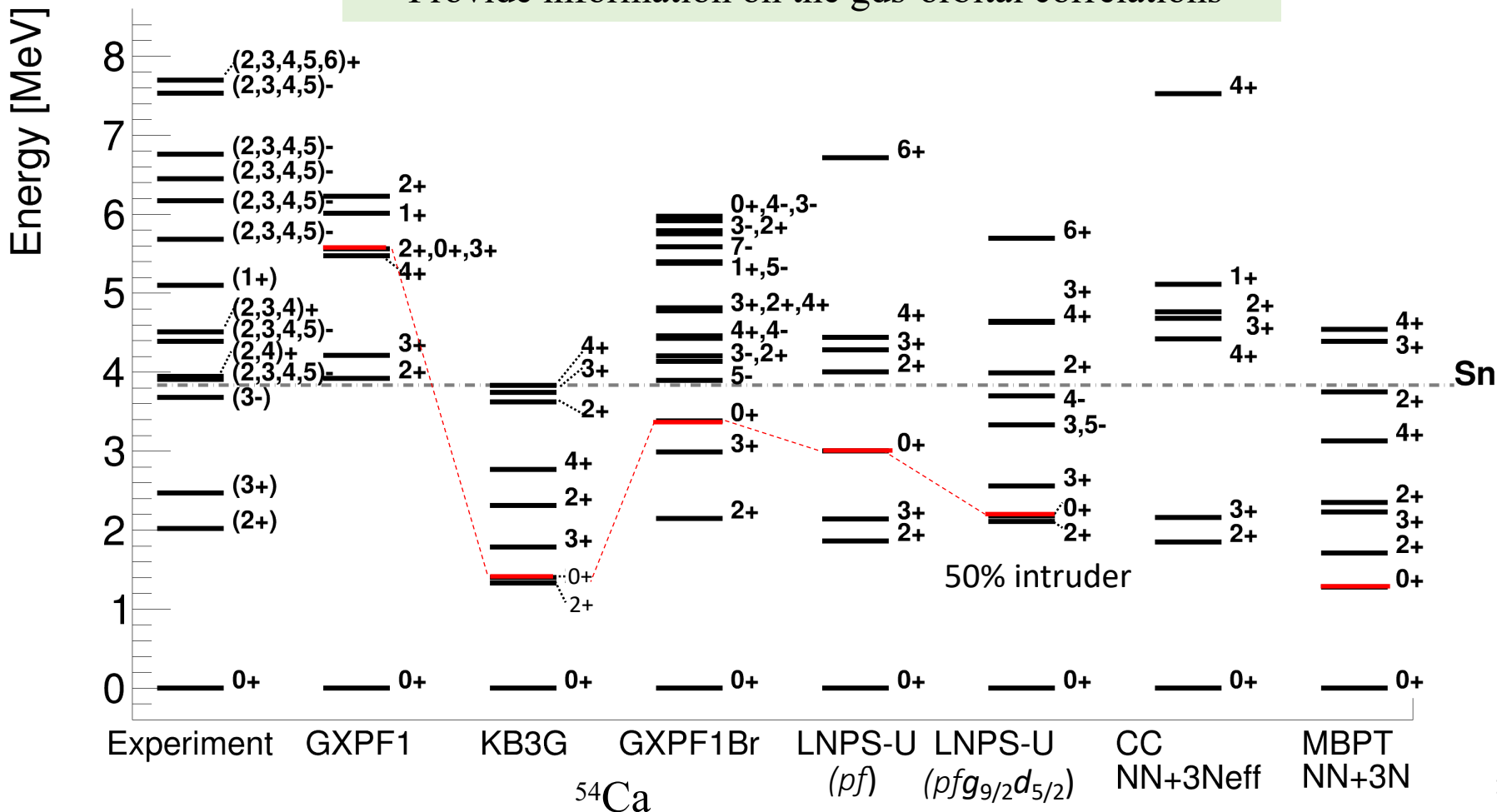
Theoretical predictions for ^{54}Ca

Exp.: F. Browne et al., PRL 126(2021); Unpublished data from SEASTAR3;

Theory: MBPT: J. D. Holt et al., PRC, 90 (2014); CC.: G. Hagen et al., PRL109 (2012)

GXPF1Br: Y. Utsuno (2020); LNPS-U: A. Poves and F. Nowacki (2020)

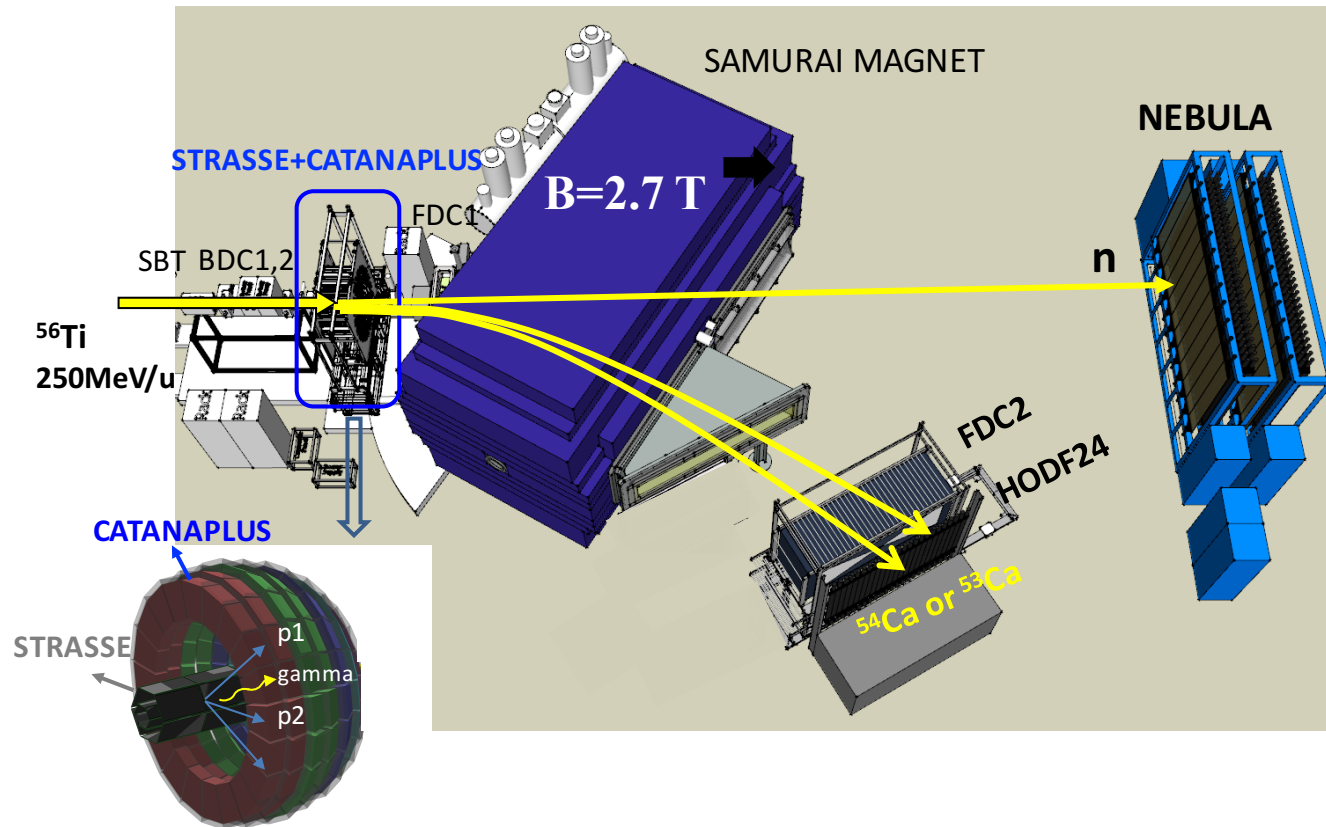
- ✓ Predicted $E(0_2^+)$ in ^{54}Ca diverges significantly
- ✓ Provide information on the gds-orbital correlations



Approved exp. @ RIBF to evidence the 0_2^+ state in ^{54}Ca via $^{56}\text{Ti}(\text{p},3\text{p})$

SEASTAR3	Exp.	$^{56}\text{Ti}(\text{p},3\text{p})^{54}\text{Ca}$	0_1^+	0_2^+	2_1^+	3_1^-
$^{54}\text{Ca}(\text{p},3\text{p})^{52}\text{Ar}$ $\sigma_{\text{incl.}}$	0.048(6) mb	GXP1Br	0.018 mb	0.011 mb	0.008 mb	0.015 mb
$^{52}\text{Ca}(\text{p},3\text{p})^{50}\text{Ar}$ $\sigma_{\text{incl.}}$	0.11(1) mb	KB3G	0.021 mb	0.023 mb	0.006 mb	--

In-beam gamma & missing-mass & invariant-mass spectroscopy



SAMURAI



STRASSE

Summary



- We performed $^{53}\text{K}(\text{p},2\text{p})^{52}\text{Ar}$ reactions to populate the excited states of ^{52}Ar at the RIBF.
- The first 2^+ state in ^{52}Ar was found at $1656(18)$ keV, the highest among the Ar isotopes with $N > 20$. Shell model calculations with phenomenological and chiral-effective-field-theory interactions both provide an overall good agreement with the data and support a robust $N=34$ subshell closure in ^{52}Ar .

H.N. Liu et al., PRL 122, 072502 (2019).

- As a next step, we will search for the 0_2^+ state in ^{54}Ca via the $^{56}\text{Ti}(\text{p},3\text{p})^{54}\text{Ca}$ reaction at the RIBF with the STRASSE+CATANAPLUS setup to study the shell evolution beyond $N = 34$.

Collaborators

L. Achouri, O. Aktas, T. Aumann, H. Baba, F. Brown, D. Calvet, F. Château, S. Chen, N. Chiga, L. Chung, M. L. Cortés, A. Delbart, P. Doornenbal, F. Flavigny, S. Franchoo, I. Gašparić, R.-B. Gerst, J.-M. Gheller, J. Gibelin, A. Gillibert, K. Hahn, C. Hilaire, D. Kim, T. Kobayashi, T. Koizumi, Y. Kondo, P. Koseglou, Y. Kubota, V. Lapoux, J. Lee, B.D. Linh, H. Liu, T. Lokotko, M. MacCormick, K. Moschner, I. Murray, A. Obertelli, H. Otsu, V. Panin, S.-Y. Park, N. Paul, W. Rodriguez, E. Sahin, M. Sasano, P.-A. Söderström, D. Sohler, D. Steppenbeck, L. Stuhl, Y. Sun, S. Takeuchi, Y. Togano, H. Törnqvist, V. Vaquero, S. Wang, V. Werner, K. Wimmer, H. Yamada, D. Yan, Z. Yang, M. Yasuda and L. Zanetti

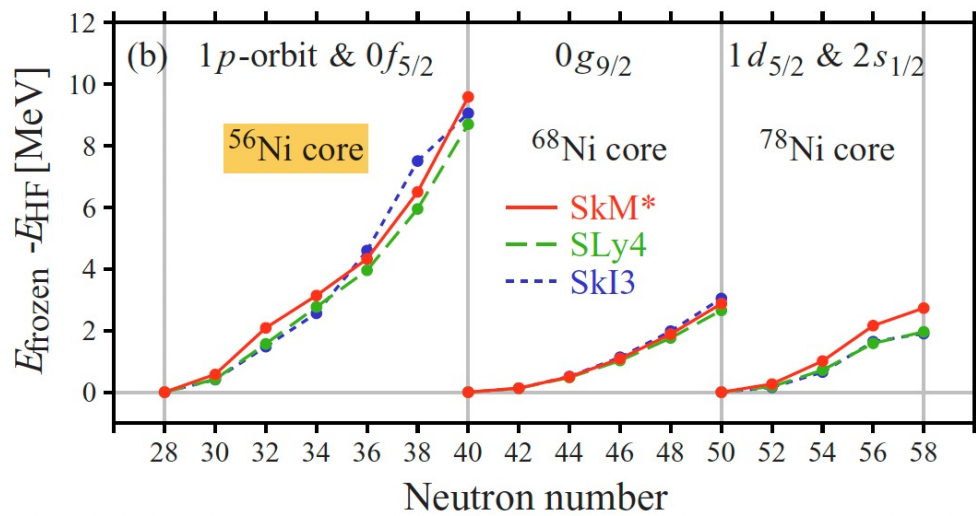
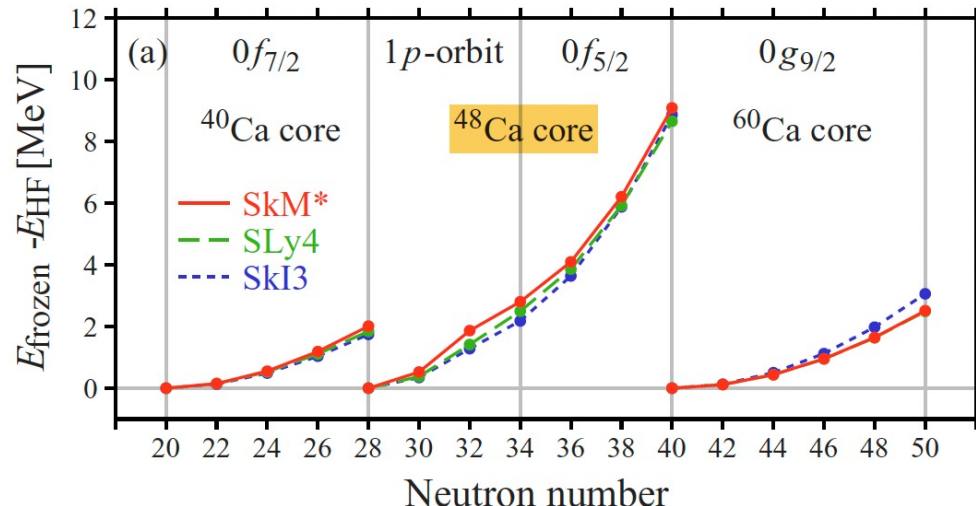


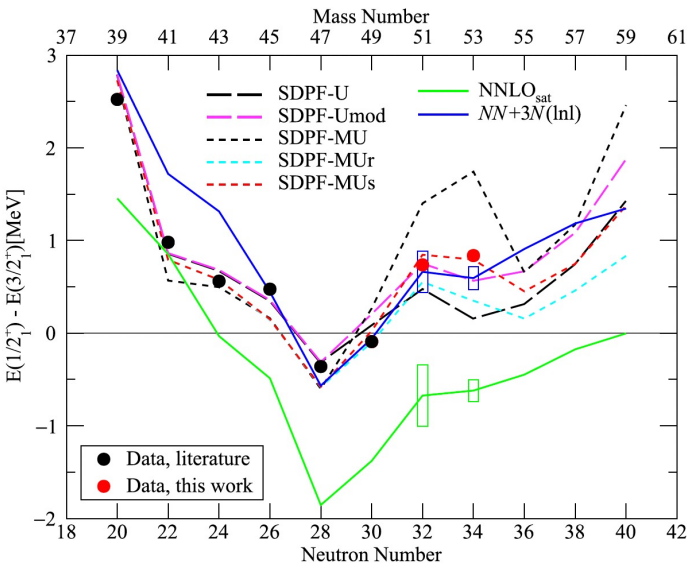
Theory: C.A. Bertulani, G. Hagen, J.D. Holt,
G.R. Jansen, T.D. Morris, A. Schwenk, R. Stroberg

Backup slides

Swelling core in spherical nuclei

PHYSICAL REVIEW C 101, 061301(R) (2020)



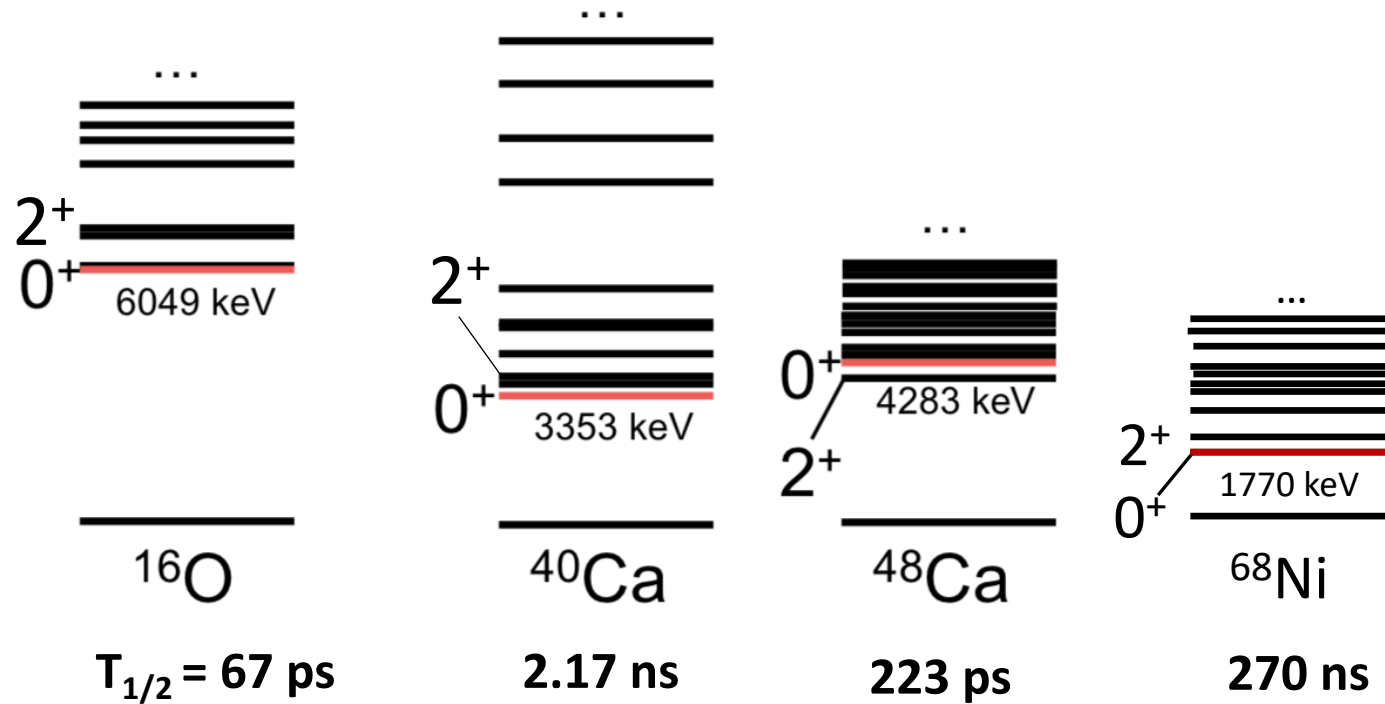


	E_{exp} (keV)	J^π	σ_{exp} (mb)	E_{th} (keV)			J^π	SF _{th}			σ_{sp} (mb)	σ_{th} (mb)		
				Th.1	Th.2	Th.3		Th.1	Th.2	Th.3		Th.1	Th.2	Th.3
⁵¹ K	0	$3/2^+$	5.2(4)	0	0	0	$3/2^+$	2.76	3.65	3.53	1.73	4.77	6.31	6.11
	737(5)	$1/2^+$	1.7(2)	883	747	846	$1/2^+$	1.27	1.68	1.59	1.88	2.39	3.16	2.99
⁵³ K	0	$3/2^+$	3.8(3)	0	0	0	$3/2^+$	2.90	3.80	3.71	1.49	4.32	5.66	5.53
	837(5)	$1/2^+$	1.5(2)	717	560	794	$1/2^+$	1.36	1.74	1.66	1.64	2.23	2.85	2.72

Experiment	J^π			σ_{sp}	LSSM		VS-IMSRG		SCGF NNLO _{sat}		SCGF NN+3N(lnl)	
	E (keV)	σ (mb)	C^2S		E (keV)	C^2S	E (keV)	C^2S	E (keV)	C^2S	E (keV)	C^2S
⁵⁶ Ca($p, 2p$) ⁵⁵ K												
0	3.5(7)	3.09(62)	$3/2^+$	1.15	0	3.08	0	2.88	252	2.35	0	3.02
668(10)	1.7(5)	1.31(42)	$1/2^+$	1.30	451	1.06	200	1.24	0	1.25	966	1.52

First excited 0^+ states in doubly-magic nuclei

- Low-lying 0^+ states are a feature of closed shell nuclei.
- It is key to understand their structure: configuration mixing and shape coexistence
- They often decay via pair production, with a(n inconvenient) lifetime of few ns



Experimental data from NNDC

